A GLOBAL GEOLOGICAL MAP OF PLUTO AT 1:7M SCALE. O. L. White[1,2], K. N. Singer[3], D. A. Williams[4], J. M. Moore[2], R. M. C. Lopes[5]. [1]SETI Institute, Mountain View, CA, 94043 (owhite@seti.org), [2]NASA Ames Research Center, Moffett Field, CA, 94035, [3]Southwest Research Institute, Boulder, CO, 80302, [4]Arizona State University, Tempe, AZ, 85281, [5]NASA Jet Propulsion Laboratory, Caltech, Pasadena, CA, 91109.

Introduction: Following its flyby of the Pluto system in 2015, NASA's *New Horizons* spacecraft returned high quality images revealing an unexpectedly diverse range of landscapes on Pluto [1,2]. Pluto's terrains exhibit highly disparate morphologies and crater spatial densities [3,4], implying a complex geological history. Surface renewal is ongoing, as demonstrated most compellingly by the nitrogen ice plains of Sputnik Planitia [5]. Pluto's geology displays evidence for having been affected by both endogenic and exogenic energy sources, and its complex nature is likely caused by combinations of these influences governing the distribution and behavior of different surface compositional suites to strongly varying degrees across even small lateral distances.

We have used established planetary geologic mapping techniques [6] to produce a first draft of a global geologic map at 1:7M scale (at the equator) for the >75% of Pluto's surface that was imaged by *New Horizons*, and which will be published as a US Geological Survey Scientific Investigations Map (SIM). This map will represent a critical tool for resolving differing hypotheses of Pluto's evolution.

Technical approach: The base map consists of a mosaic of New Horizons images ranging between 234 m/pixel and 40.6 km/pixel. A consequence of the flyby nature of the *New Horizons* mission is that the spacecraft only obtained high-resolution coverage of the anti-Charon hemisphere of Pluto (the "near side"). The sub-Charon hemisphere (the "far side") was imaged at much lower resolution, and so has necessarily been mapped at a much coarser scale, with separate units being defined for the near side and far side (even though some far side units are interpreted to have direct analogues on the near side). Another consequence is that, for the near side, each point on the surface was only imaged at a single solar incidence and emission angle, with these parameters varying from 0° to 90° across the mapping area, which must be accounted for in order to ensure consistency in unit definition. Along the southern margin of the near side is a 350 km wide strip that was beyond the terminator during flyby, but within which terrain could still be dimly discerned owing to scattering of light by haze in Pluto's atmosphere. The southernmost portions of the near side and far side have been left unmapped owing to poor image quality. A stereo digital elevation model of Pluto that is projected at 300 m/pixel [7] allows topographic features as small as a few kilometers across to be resolved, and is an essential resource for assessing the relief and relative elevations of our mapped units, which aids in the interpretation of their formation and determination of their stratigraphy. We also employ color and compositional maps as an additional resource for unit definition and interpretation [7,8].

Mapping results: The geological map is shown in Fig. 1. 45 units have been mapped, including 7 on the far side, as have tectonic lineations (all extensional in nature) and the troughs separating convection cells in Sputnik Planitia. Impact craters >25 km in diameter have been mapped as the bright yellow unit, and those between 7 and 25 km diameter as point features. Six geological groups have been identified, each consisting of units that represent a major episode of geological activity on Pluto's surface. The interpreted chronological order from youngest to oldest is Sputnik (~3 Ma), Wright (<2 Ga), Tartarus (>2 Ga), Hayabusa (<4 Ga), Venera (~4 Ga), and Burney (≥4 Ga). Fig. 2 shows the stratigraphic correlation of mapped units. Relative ages are derived from superposition relations and crater statistics, with crater flux models [4,9] being used to assign rough absolute age ranges for units.

The wide range of surface ages displayed by the groups appears to be primarily a consequence of how surface volatile distribution is affected by atmospheric, geographic, and topographic effects. There is a gradual transition across the far side from ancient, volatile-poor, cratered, and glaciated terrains west of Sputnik Planitia (the Burney and Venera groups), to young, volatile-rich terrains consisting of thick methane ice-based deposits to its east (the Tartarus and Hayabusa groups). This illustrates the power of Sputnik Planitia, Pluto's prime repository of surface nitrogen ice (the Sputnik group) that is contained within an ancient, deep impact basin [2,5,7], to regulate atmospheric circulation [10] and the longitudinal distribution of volatiles. Furthermore, the greater contrast between volatile-rich and volatile-poor terrains in the permanently diurnal equatorial regions compared to those in the arctic mid-latitudes, while the north polar region appears volatile-poor and ancient, reflects an additional geographical control on volatile stability and distribution by Pluto's distinct climate zones that stem from its high obliquity (which ranges between 103° and 127°) [11,12]. The extremely young surface age of the Sputnik group itself can be attributed to ongoing solid-state convection [5], glacial flow [13], and sublimation and deposition of the ice.

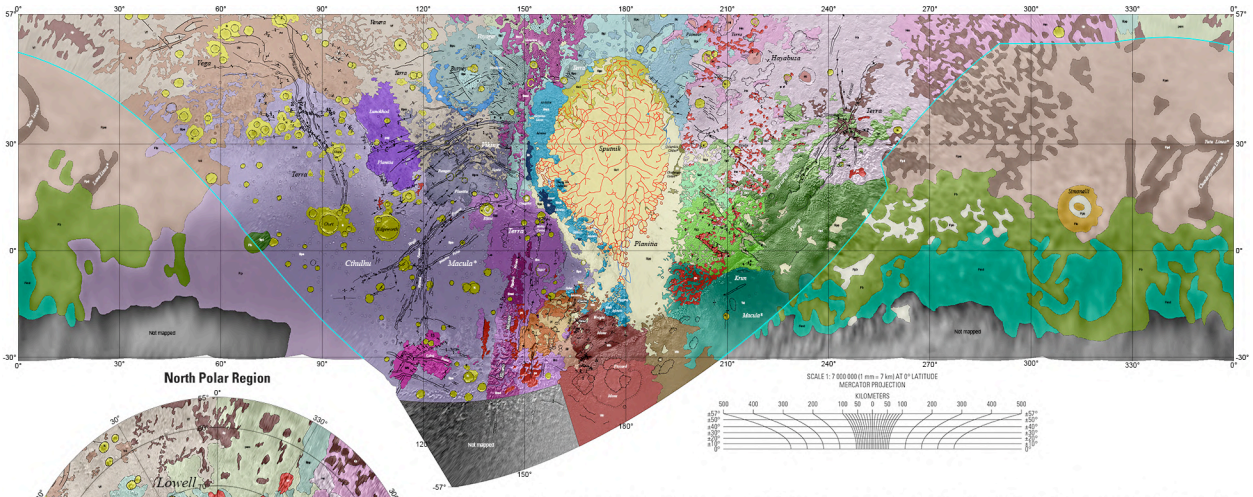

Figure 1. Geological map of Pluto, presented in Mercator projection between 50°S and 57°N, and polar stereographic projection north of 55°N. Cyan line indicates the boundary between the near and far sides. Tectonic lineations, scarp crests, crater rim crests, and depression margins are mapped as black lines, and troughs within Sputnik Planitia as red lines. The Sputnik group consists of yellow-colored units in the center of the map; the Wright group of red/brown-colored units south of Sputnik; the Tartarus group of green-colored units east of Sputnik; the Hayabusa group of pink-colored units northeast of Sputnik; the Venera group of beige-colored units northwest of Sputnik; and the Burney group of blue/purple-colored units west and north of Sputnik, and in the north polar region. Feature names marked with a * are informal.

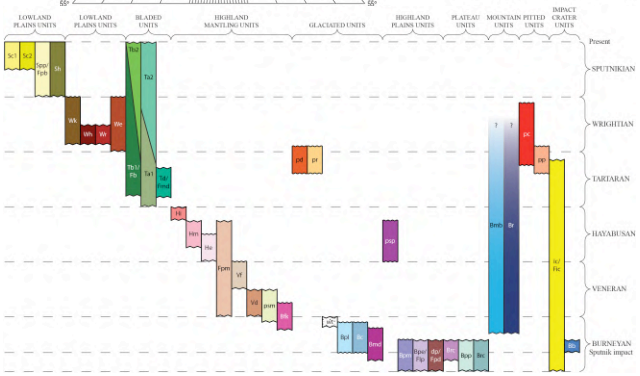

Figure 2. Correlation of map units, with younger units at the top and older at the bottom. The vertical location and extent of each bar provides an interpretation about the nature of temporal sequencing between units, and the onset and cessation of the geological event that produced each unit. Unit boxes that are contiguous indicate a close formative association.

Onto this global pattern are superimposed endogenic effects of widely differing ages. These include the quite recent terrains of the Wright group that are tentatively interpreted as cryovolcanic, on account of the large mounds (Wright and Piccard Montes) with enormous central depressions and a hummocky texture that form the centerpiece of the Wright group. By contrast, the NNE-SSW-aligned ridge-trough system that traverses virtually the entire near side (purple units west of Sputnik Planitia and in the north polar region), is the largest and most ancient tectonic system yet seen on Pluto: a complex, eroded, and cratered band of graben, troughs, ridges, plateaus, tilted blocks, and elongate depressions that may even predate the Sputnik basin-forming impact [7].

Acknowledgements: This research has been funded by NASA's PDART program.

References: [1] Stern S. A. et al. (2018) *Annu. Rev. Astron. Astrophys.*, *56*, 357-392. [2] Moore J. M. et al. (2016) *Science*, *351*, aad7055. [3] Robbins S. J. et al. (2017) *Icarus*, *287*, 187-206. [4] Singer K. N. et al. (2019) *Science*, *363*, 955-959. [5] McKinnon W. B. et al. (2016) *Nature*, *534*, 82-85. [6] Skinner J. A. et al. (2018) *Planetary Geologic Mapping Protocol-2018*. USGS, Flagstaff, AZ. [7] Schenk P. M. et al. (2018) *Icarus*, *314*, 400-433. [8] Schmitt B. et al. (2017) *Icarus*, *287*, 229-260. [9] Greenstreet S. et al. (2015) *Icarus*, *258*, 267-288. [10] Bertrand T. et al. (2020) *J. Geophys. Res. Planets*, *125*, e2019JE006120. [11] Binzel R. P. et al. (2017) *Icarus*, *287*, 30-36. [12] Earle A. M. et al. (2018) *Icarus*, *303*, 1-9. [13] Umurhan O. M. et al. (2017) *Icarus*, *287*, 301-319.